Inorg. Chem. **2004**, *43*, 4400–4405

Zr_7Sb_4: A New Binary Zirconium-Rich Antimonide

Andriy V. Tkachuk and Arthur Mar*

Department of Chemistry, University of Alberta, Edmonton, Alberta, Canada T6G 2G2

Received March 3, 2004

Zr_7Sb_4 has been prepared by arc-melting of the elemental components and annealing at 1000–1150 °C. Its crystal structure was determined by X-ray diffraction (Pearson symbol *mP*44, monoclinic, space group $P2_1/c$, $Z = 4$, $a = 8.4905(6)$ Å, $b = 11.1557(8)$ Å, $c = 11.1217(8)$ Å, $\beta = 111.443(2)°$ at 295 K). Zr_7Sb_4 is isotypic to Hf_6TiSb_4, a compound stabilized by differential fractional site occupancy. It is the first binary group-4 antimonide with this metal-to-antimony ratio, but it differs from the corresponding phosphides and arsenides M_7Pn_4 (M = Ti, Zr, Hf; Pn = P, As), which adopt the Nb_7P_4-type structure. Zr_7Sb_4 is built up from layers excised from the tetragonal W_5Si_3-type structure; these layers are displaced relative to each other to maximize interlayer Zr–Zr and Zr–Sb bonding, as confirmed by band structure calculations.

Introduction

Binary pnictides of the group-4 transition metals exhibit a remarkably complex structural chemistry that is still not fully elucidated to this day. Among group-4 pnictides with the formula M_7Pn_4 (M = Ti, Zr, Hf; Pn = pnicogen), the phases Ti_7P_4,[1] Zr_7P_4,[2,3] Hf_7P_4,[4] Zr_7As_4,[3] and Hf_7As_4 [5] have been identified, all adopting the Nb_7P_4-type structure.[6] None of the corresponding antimonides has been reported, but the expectation is that they would not be isostructural to the phosphides or arsenides. The apparent absence of "Zr_7Sb_4" is striking, given that the Zr−Sb system abounds with compounds, ranging from Zr_3Sb, the most metal-rich phase, to what were previously described as two forms of $ZrSb_2$,[7−9] the most antimony-rich phases (the existence of "β-$ZrSb_2$" has been recently challenged).[10] However, the characterization of this system is far from complete, as exemplified by the recent discovery of the latest member, $Zr_{11}Sb_{18}$,[11] and by allusion to the existence of a phase "Zr_2Sb" of unknown structure.[7,9] The mixed antimonide−selenide, $Zr_7(Sb_{1.6}Se_{2.4})$, has been described to be stabilized by anionic differential fractional site occupancy (DFSO), adopting a polar variant of the Nb_7P_4-type structure.[12] Similarly, Hf_6TiSb_4 has been considered to be a cationic DFSO-stabilized compound, adopting a unique monoclinic structure type.[13] The criteria for a cationic (anionic) DFSO-stabilized compound are that all metal (nonmetal) sites are fractionally occupied by mixtures of atoms that are fixed at each site but vary from site to site, and that it possesses a different structure from either of the parent binary compounds, if they exist at all.[14,15]

We report here the synthesis of the long-sought binary zirconium antimonide Zr_7Sb_4, which adopts the same structure as Hf_6TiSb_4. In a revised interpretation, we argue that this structure is built up from layers that are fragments of the W_5Si_3-type structure.[16] By evaluating the degree of interlayer bonding with the use of band structure calculations, we show that this point of view provides insight into why the layers are shifted relative to each other.

Experimental Section

Synthesis. Starting materials were powders of zirconium (99.7%, Cerac) and antimony (99.995%, Aldrich). In a Centorr 5TA tri-arc furnace under high-purity argon gettered with Ti, Zr_7Sb_4 was prepared by arc-melting cold-pressed pellets (~0.25 g) of the elemental components, with an excess of 2.5 wt % Sb added to

* To whom correspondence should be addressed. E-mail: arthur.mar@ualberta.ca.

(1) Carrillo-Cabrera, W. *Acta Chem. Scand., Ser. A* **1982**, *36*, 563−570.
(2) Ahlzén, P.-J.; Rundqvist, S. *Z. Kristallogr.* **1989**, *189*, 149−153.
(3) Willerström, J.-O. *Acta Chem. Scand., Ser. A* **1984**, *38*, 91−93.
(4) Kleinke, H.; Franzen, H. F. *Angew. Chem., Int. Ed. Engl.* **1996**, *35*, 1934−1936.
(5) Rundqvist, S.; Carlsson, B. *Acta Chem. Scand.* **1968**, *22*, 2395−2396.
(6) Rundqvist, S. *Acta Chem. Scand.* **1966**, *20*, 2427−2434.
(7) Garcia, E.; Corbett, J. D. *J. Solid State Chem.* **1988**, *73*, 440−451.
(8) Garcia, E.; Corbett, J. D. *J. Solid State Chem.* **1988**, *73*, 452−467.
(9) Rossteutscher, W.; Schubert, K. *Z. Metallkd.* **1965**, *56*, 813−822.
(10) Soheilnia, N.; Assoud, A.; Kleinke, H. *Inorg. Chem.* **2003**, *42*, 7319−7325.
(11) Elder, I.; Lee, C.-S.; Kleinke, H. *Inorg. Chem.* **2002**, *41*, 538−545.
(12) Kleinke, H.; Harbrecht, B. *Z. Anorg. Allg. Chem.* **1999**, *625*, 1873−1877.
(13) Kleinke, H. *Inorg. Chem.* **1999**, *38*, 2931−2935.
(14) Kleinke, H. *Trends Inorg. Chem.* **2001**, *7*, 135−149.
(15) Franzen, H. F.; Köckerling, M. *Prog. Solid State Chem.* **1995**, *23*, 265−289.
(16) Aronsson, B. *Acta Chem. Scand.* **1955**, *9*, 1107−1110.

10.1021/ic040034y CCC: $27.50
Published on Web 06/11/2004

Table 1. Crystallographic Data for Zr_7Sb_4

chemical formula = $Zr_7Sb_{3.935(3)}$	fw =1116.41
$a = 8.4905(6)$ Å	space group C_{2h}^5−$P2_1/c$ (No. 14)
$b = 11.1557(8)$ Å	$T = 22$ °C
$c = 11.1217(8)$ Å	$\lambda = 0.710\ 73$ Å
$\beta = 111.443(2)°$	$\rho_{calcd} = 7.563$ g cm^{-3}
$V = 980.50(12)$ Å^3	μ(Mo Kα) = 176.54 cm^{-1}
$Z = 4$	$R(F)$ for $F_o^2 > 2\sigma(F_o^2) = 0.040^a$
	$R_w(F_o^2) = 0.082^b$

^{a} $R(F) = \sum||F_o| - |F_c||/\sum|F_o|$. ^{b} $R_w(F_o^2) = [\sum[w(F_o^2 - F_c^2)^2]/\sum wF_o^4]^{1/2}$; $w^{-1} = [\sigma^2(F_o^2) + (0.0320p)^2 + 8.5859p]$ where $p = [\max(F_o^2, 0) + 2F_c^2]/3$.

compensate for evaporation loss. The alloys were then sealed in evacuated fused-silica tubes and annealed successively at 1000, 1100, and 1150 °C for 48 h at each temperature. After the heat treatment, the ingots were quenched in cold water. The arc-melted ingots of the ternary compound have a metallic luster, and the powders are gray and are stable in air. The products were characterized by powder X-ray diffraction on an Enraf-Nonius FR552 Guinier camera, recorded with Cu Kα_1 radiation (λ = 1.54056 Å) using silicon as an external standard. The monoclinic cell parameters refined by analysis of the powder X-ray data were $a = 8.414(7)$ Å, $b = 11.164(9)$ Å, $c = 11.098(6)$ Å, $\beta = 111.89(5)°$, and $V = 967.2(8)$ Å^3. There does not appear to be a significant phase width, but this is difficult to determine definitively because the composition of Zr_7Sb_4 is very close to that of the nearby phases Zr_5Sb_3 and Zr_2Sb, and because loss of Sb occurs during the arc-melting.

Single crystals of Zr_7Sb_4 were isolated from crushed samples after the 1000 °C annealing. Energy-dispersive X-ray (EDX) analysis of selected single crystals on a Hitachi S-2700 scanning electron microscope gave a composition of 61% Zr and 39% Sb (mol %), in good agreement with the expected values of 64% Zr and 36% Sb, and did not reveal the presence of any impurity elements.

Structure Determination. Intensity data were collected on a Bruker Platform/SMART 1000 CCD diffractometer at 22 °C using ω scans (0.2°). Crystal data are given in Table 1. Calculations were carried out with use of the SHELXTL (version 5.1) package.[17] Face-indexed numerical absorption corrections were applied. The intensity symmetry and the systematic absences are consistent uniquely with the centrosymmetric monoclinic space group $P2_1/c$. Initial positions for all atoms were located by direct methods, and the structure was refined by full-matrix least-squares methods on F^2 with anisotropic displacement parameters. Refinements on the occupancy factors confirmed that all the sites are fully occupied except for Sb1, which has an occupancy of 93.5(3)%, resulting in the formula $Zr_7Sb_{3.935(3)}$. No extraneous elements were found within the detection limits of the EDX analysis on numerous samples (including the crystal selected for structure determination), and no attack of the silica tubes was visible in the reactions from which these crystals were selected, supporting our assertion that this is a binary phase. However, given that "β-$ZrSb_2$" was recently suggested to be stabilized by small amounts of Si impurities,[10] we considered a model in which the partially occupied Sb1 site contains instead a mixture of Si and Sb atoms. A refinement of this model leads to the formula "$Zr_7Si_{0.09(1)}Sb_{3.91(1)}$", corresponding to a 1 mol % impurity level of Si, which is near the detection limits of the EDX analysis, although other sources of systematic error (such as absorption corrections) could well influence the validity of this formula. For simplicity, we refer to the fully stoichiometric formula Zr_7Sb_4. The final refinement led to reasonable displacement parameters and a featureless difference electron density map. The atomic positions were standardized with the program STRUCTURE TIDY.[18] Positional and displacement parameters are given in Table 2, and interatomic distances are listed in Table 3. Further data are available as Supporting Information.

Table 2. Positional and Equivalent Isotropic Displacement Parameters for Zr_7Sb_4

atom^a	x	y	z	U_{eq} (Å^2)^b
Zr1	0.01109(10)	0.42349(6)	0.21020(7)	0.0079(1)
Zr2	0.01268(10)	0.20432(7)	0.43250(7)	0.0087(1)
Zr3	0.20032(10)	0.50037(7)	0.55485(7)	0.0090(1)
Zr4	0.34167(10)	0.73888(6)	0.01876(7)	0.0076(1)
Zr5	0.35751(10)	0.27756(7)	0.17236(7)	0.0082(1)
Zr6	0.36773(10)	0.05642(6)	0.36399(7)	0.0084(1)
Zr7	0.60147(10)	0.05741(7)	0.15904(7)	0.0097(1)
Sb1^c	0.01037(8)	0.15557(5)	0.16265(5)	0.0111(2)
Sb2	0.22988(7)	0.50747(4)	0.06190(5)	0.0077(1)
Sb3	0.31625(7)	0.32118(4)	0.41917(5)	0.0092(1)
Sb4	0.71701(7)	0.31428(4)	0.24786(5)	0.0089(1)

^{a} All atoms in Wyckoff position 4e. ^{b} U_{eq} is defined as one-third of the trace of the orthogonalized $\mathbf{U}_{ij}$ tensor. ^{c} Occupancy 0.935(3).

Band Structure. Tight-binding extended Hückel band structure calculations were performed with use of the EHMACC suite of programs.[19,20] The atomic parameters are listed in Table 4. Properties were extracted from the band structure using 120 k-points in the irreducible portion of the Brillouin zone.

Results and Discussion

Synthesis. Zr_7Sb_4 is a new phase in the Zr−Sb system, in a region of the phase diagram where there is still much ambiguity. Near the composition of Zr_7Sb_4, two modifications each of Zr_2Sb (La_2Sb-type and another of unknown structure (X-type)) and Zr_5Sb_{3+x} (Yb_5Bi_3- and Mn_5Si_3-types) have been previously identified.[7] Zr_7Sb_4 is stable only within a narrow temperature range. Annealing the arc-melted pellet between 1000 and 1150 °C yields phase-pure product. Below 1000 °C, Zr_5Sb_3 (Yb_5Bi_3-type) and traces of Zr_2Sb (La_2Sb-type) are formed, whereas at 1200 °C, Zr_5Sb_3 (Yb_5Bi_3-type) and minor amounts of Zr_3Sb (Ni_3P-type) are formed. Although annealed at similar temperatures, Zr_7Sb_4 does not appear to be related to the X-phase of Zr_2Sb, as revealed by comparison of their X-ray diffraction patterns. Attempts were made to prepare the analogous hafnium-containing phase, Hf_7Sb_4. Annealing at 900−1200 °C resulted predominantly in Hf_5Sb_3 (Yb_5Bi_3-type) and possibly traces of Hf_7Sb_4, although the evidence is not definitive. It is likely, as others have pointed out, that the sequence of heat treatment can have a profound impact on what products are formed.[7]

Structure. Zr_7Sb_4 is isostructural to Hf_6TiSb_4, a structure type that was recently argued to be unique and stabilized by mixed Hf/Ti occupancies.[13] It is possible to build up the three-dimensional structure from a stacking of two kinds of layers along the a-direction: a layer A of metal and Sb atoms at $x = 0$, and a double layer B of metal atoms at $x = {}^1/_2$. As

(17) Sheldrick, G. M. *SHELXTL*, version 5.1; Bruker Analytical X-ray Systems, Inc.: Madison, WI, 1997.

(18) Gelato, L. M.; Parthé, E. *J. Appl. Crystallogr.* **1987**, *20*, 139−143.

(19) Whangbo, M.-H.; Hoffmann, R. *J. Am. Chem. Soc.* **1978**, *100*, 6093−6098.

(20) Hoffmann, R. *Solids and Surfaces: A Chemist's View of Bonding in Extended Structures*; VCH Publishers: New York, 1988.

Table 3. Interatomic Distances (Å) Shorter Than 4 Å in Zr_7Sb_4 [a]

	Zr1	Zr2	Zr3	Zr4	Zr5	Zr6	Zr7	Sb1	Sb2	Sb3	Sb4
Zr1		3.4062	3.6752	3.6277	3.5190	3.3593	3.4162	2.9873	3.0479	3.0024	2.9425
		3.4736	3.7683					3.0349	3.0676		
		3.4843									
Zr2	3.4062		3.7030	3.2690	3.1652	3.7510		3.0053	3.0189	2.9401	2.8731
	3.4736		3.7854					3.0431	3.0268		
	3.4843										
Zr3	3.6752	3.7030	3.1663	3.2271	3.4391	3.2664	**3.2362**	2.9118		2.8859	2.9080
	3.7683	3.7854					3.4384	2.9808			
Zr4	3.6277	3.2690	3.2271		**3.4778**	**3.0950**	3.1632	3.1594	2.8510	**2.8791**	2.8832
					3.8788	3.7607	3.9884				2.9391
Zr5	3.5190	3.1652	3.4391	**3.4778**		3.2405	**3.2509**	3.2122	2.8790	2.9230	**2.8837**
				3.8788		3.9265	3.5925			2.9321	
						3.9966					
Zr6	3.3593	3.7510	3.2664	**3.0950**	3.2405	**3.2884**	**3.5273**	3.2367	2.9336	3.0802	2.9508
				3.7607	3.9265				**3.2543**		
					3.9966						
Zr7	3.4162		**3.2362**	3.1632	**3.2509**	**3.5273**	**3.5591**	3.6265	2.9570	2.9383	3.0726
			3.4384	3.9884	3.5925					**3.1768**	
Sb1	2.9873	3.0053	2.9118	3.1594	3.2122	3.2367	3.6265			3.5889	3.4587
	3.0349	3.0431	2.9808								
Sb2	3.0479	3.0189		2.8510	2.8790	2.9336	2.9570		3.6376		3.9620
	3.0676	3.0268				**3.2543**					
Sb3	3.0024	2.9401	2.8859	**2.8791**	2.9230	3.0802	2.9383	3.5889			
					2.9321		**3.1768**				
Sb4	2.9425	2.8731	2.9080	2.8832	**2.8837**	2.9508	3.0726	3.4587	3.9620		
				2.9391							

[a] Standard uncertainties of ~0.0010 Å. Interlayer contacts are highlighted in bold.

Table 4. Extended Hückel Parameters

atom	orbital	H_{ii} (eV)	ζ_{i1}	c_1	ζ_{i2}	c_2
Zr	5s	−8.52	1.82			
	5p	−4.92	1.78			
	4d	−8.63	3.84	0.621	1.510	0.579
Sb	5s	−18.8	2.32			
	5p	−11.7	2.00			

structural systematization is an important aim in solid-state chemistry, we propose here an alternative and perhaps more elegant description that is based on the presence of condensed metal clusters, a theme that pervades many metal-rich compounds of the early transition metals.[21] Figure 1 shows that Zr_7Sb_4 consists of finite dimeric clusters: face-sharing Zr square antiprisms centered by Sb atoms, $[Zr_{12}Sb_2]$, and edge-sharing Sb tetrahedra centered by Zr atoms, $[Sb_6Zr_2]$. These two types of clusters are arranged in a checkerboard fashion within the *bc* plane, forming a layer of composition $[Zr_{12}Sb_2] + [Sb_6Zr_2] = {}^2_\infty[Zr_{14}Sb_8]$ or ${}^2_\infty[Zr_7Sb_4]$. Successive layers are then slipped as they are stacked on top of each other.

This description draws attention to the close relationship of Zr_7Sb_4 to the W_5Si_3-type structure, an important one adopted by many intermetallic compounds.[16] As shown in Figure 2, the W_5Si_3-type structure is built up from similar kinds of square antiprismatic and tetrahedral clusters as in Zr_7Sb_4, but condensed to form infinite columns ${}^1_\infty[M_{8/2}X]$ and ${}^1_\infty[X_{4/2}M]$. The structure of Zr_7Sb_4 can then be regarded as comprising two-slab-thick fragments of W_5Si_3. (Alternatively, it results from removing every third interstitial atom in the infinite columns, $3 \times M_5X_3 = M_{15}X_9 \xrightarrow{-M,-X} M_{14}X_8 = 2 \times M_7X_4$.) These fragment layers are displaced by a shift Δ with respect to each other.

This picture does not imply that the bonding between the clusters within a layer or between layers is weak. For

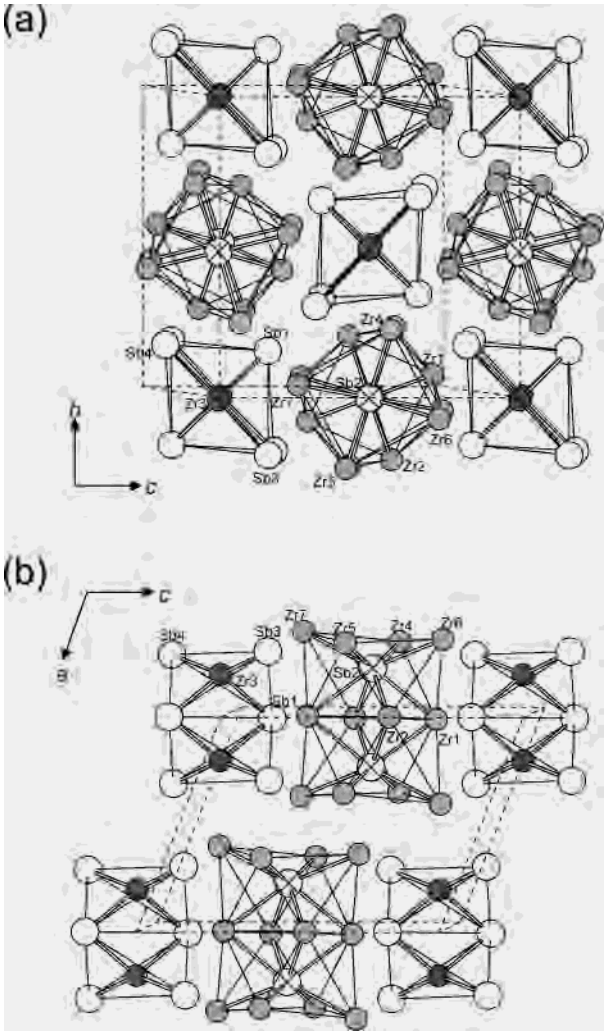

Figure 1. Structure of Zr_7Sb_4 in terms of square antiprismatic and tetrahedral clusters, shown as bounded projections at (a) $-1/2 < x < 1/2$ and (b) $-1/4 < y < 1/4$. The shaded circles are Zr atoms and the open circles are Sb atoms.

(21) Simon, A. *Angew. Chem., Int. Ed. Engl.* **1981**, *20*, 1−22.

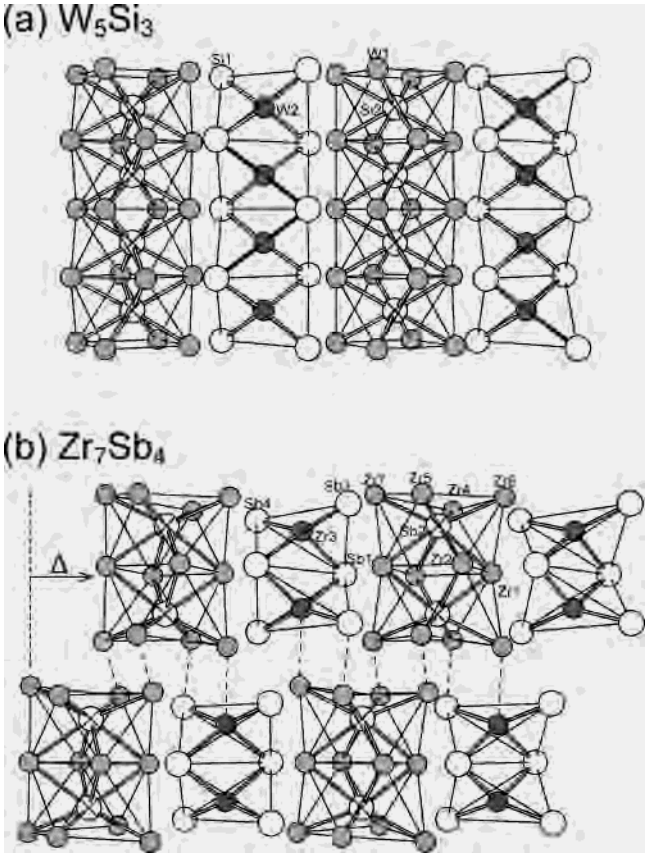

Figure 2. Comparison of the structures of (a) W_5Si_3 and (b) Zr_7Sb_4, in terms of condensed clusters. Two-slab-thick fragments of the W_5Si_3-type structure are displaced in Zr_7Sb_4 by a shift Δ.

example, the Zr−Sb distances of 2.8510(9)−3.0676(9) Å in the $[Zr_{12}Sb_2]$ cluster and 2.8859(9)−2.9808(9) Å in the $[Sb_6Zr_2]$ cluster are similar to the 2.8832(9)−3.2367(10) Å distances between clusters within a layer. Moreover, the shortest Zr−Zr contact of 3.0950(11) Å is between layers. The sums of the Pauling single-bond radii provide a basis for comparison: Zr−Sb, 2.85 Å; Zr−Zr, 2.90 Å; Sb−Sb, 2.80 Å.[22] The Zr−Sb contacts are slightly longer, 2.8510(9)−3.2543(10) Å, consistent with values found in other zirconium antimonides.[8] However, the Zr−Zr contacts are especially variable, spanning a range of shorter distances, 3.0950(11)−3.2690(11) Å, and longer ones, 3.3593(11)−3.9966(11) Å. The shorter distances are consistent with those normally found in metal-rich binary antimonides such as ZrSb (3.019(2)−3.399(1) Å),[8] but the longer ones cannot be dismissed, since values of 3.577(1)−3.684(1) Å in $Zr_{11}Sb_{18}$ have been shown to correspond to non-negligible overlap populations.[11] The surprising occurrence of Sb−Sb bonding within Hf_6TiSb_4, in the form of a nonlinear Sb_3 unit containing 3.283(7)−3.44(2) Å distances,[13] disappears on going to Zr_7Sb_4, where the Sb−Sb distances are considerably longer, 3.4587(8)−3.6376(11) Å.

Zr_7Sb_4 adopts a different structure from other group-4 pnictides Ti_7P_4, Zr_7P_4, Hf_7P_4, Zr_7As_4, and Hf_7As_4, all having the Nb_7P_4-type structure.[1−6] Nevertheless, there is some

(22) Pauling, L. *The Nature of the Chemical Bond*, 3rd ed.; Cornell University Press: Ithaca, NY, 1960.

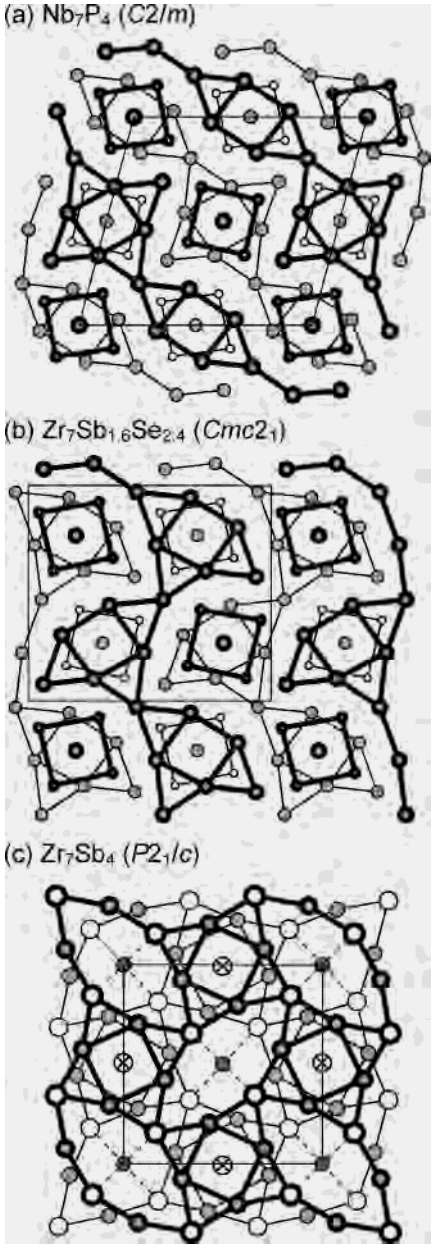

Figure 3. Comparison of the structures of (a) Nb_7P_4, (b) $Zr_7Sb_{1.6}Se_{2.4}$, and (c) Zr_7Sb_4, in terms of filled trigonal prisms. Light and heavy lines indicate that the nets of atoms lie on different planes down the projection axis. Located between the nets, a Zr atom (●) occupies a tetrahedral site, and an Sb atom (⊗) occupies a square antiprismatic site in Zr_7Sb_4.

resemblance between these structures, as shown in Figure 3. Pnicogen-centered trigonal prisms M_6Pn are a common structural motif in transition-metal pnictides, especially when the metal-to-pnicogen ratio of the compound is close to 2:1. A starlike cyclic tetramer of four connected trigonal prisms, with an additional metal atom in the body center of the resulting cube, is a characteristic building block. Nb_7P_4 is constructed from a sequence of these starlike tetramers, with two points removed in half of the tetramers.[6] $Zr_7Sb_{1.6}Se_{2.4}$ is a polar variant of Nb_7P_4, containing these tetramers with one point removed.[12] In Zr_7Sb_4, the pnicogen and one metal atom swap positions to give metal-centered trigonal prisms, Sb atoms reside in square antiprisms instead of cube body centers within the starlike tetramers, and Zr atoms fill

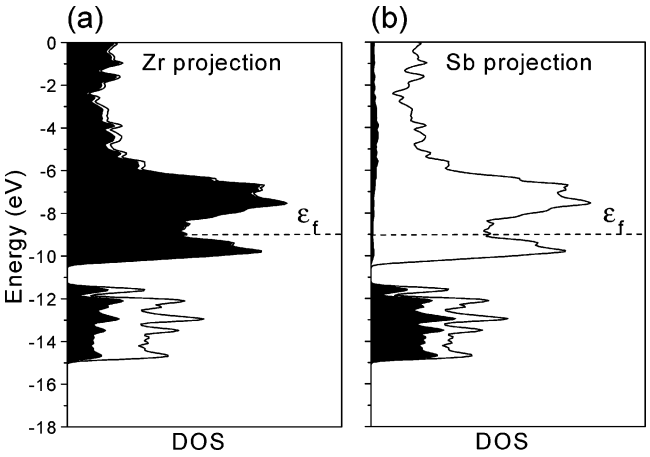

Figure 4. Contributions of (a) Zr and (b) Sb (shaded regions) to the total density of states (DOS) (line) for Zr_7Sb_4. The horizontal line marks the Fermi level ($\epsilon_f = -9.0$ eV).

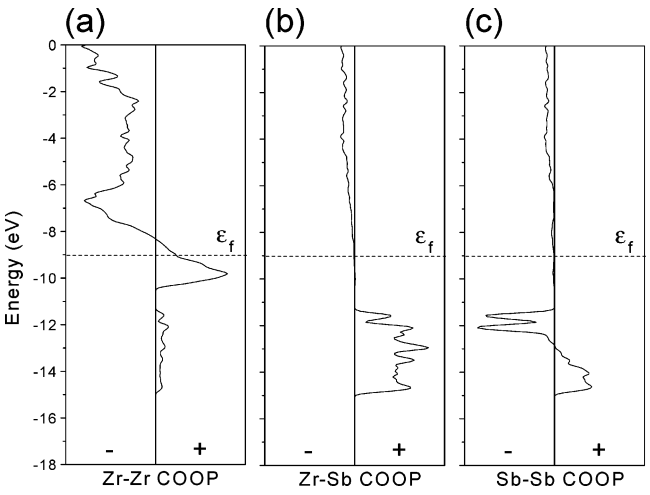

Figure 5. Crystal orbital overlap population (COOP) curves for (a) Zr−Zr, (b) Zr−Sb, and (c) Sb−Sb interactions (<4.0 Å) in Zr_7Sb_4.

tetrahedral sites between the tetramers. It would be worthwhile to re-examine the $Zr_7(Sb_{1-x}Se_x)_4$ system to determine if a transition occurs at a critical composition from the Zr_7Sb_4-type to the $Zr_7Sb_{1.6}Se_{2.4}$-type structure.

Bonding. In the absence of Sb−Sb bonding, we can begin with the assumption that electron transfer takes place from Zr to Sb, resulting in the ionic formulation $(Zr^{1.7+})_7(Sb^{3-})_4$. Even such a naive analysis suggests that metal−metal bonding must ensue through use of the 2.3 valence electrons, on average, remaining on each Zr atom. The band structure calculation reveals strong mixing of the Zr and Sb states, as shown in the density of states (DOS) curve in Figure 4, in the region between −11.1 and −15.1 eV, implying significant covalent character in the Zr−Sb bonds. There is a small band gap (0.5 eV), and then a broad, largely Zr-based manifold occurs above −10.6 eV. The Fermi level falls at −9.0 eV and crosses bands, so that metallic conduction through the Zr substructure is predicted. Most of the Sb states are occupied below the Fermi level, consistent with essentially fully reduced Sb, but there remain many unfilled Zr states. Crystal orbital overlap population (COOP) curves (for contacts less than 4.0 Å) are shown in Figure 5. Zr−Sb bonding is optimized with all bonding and no antibonding

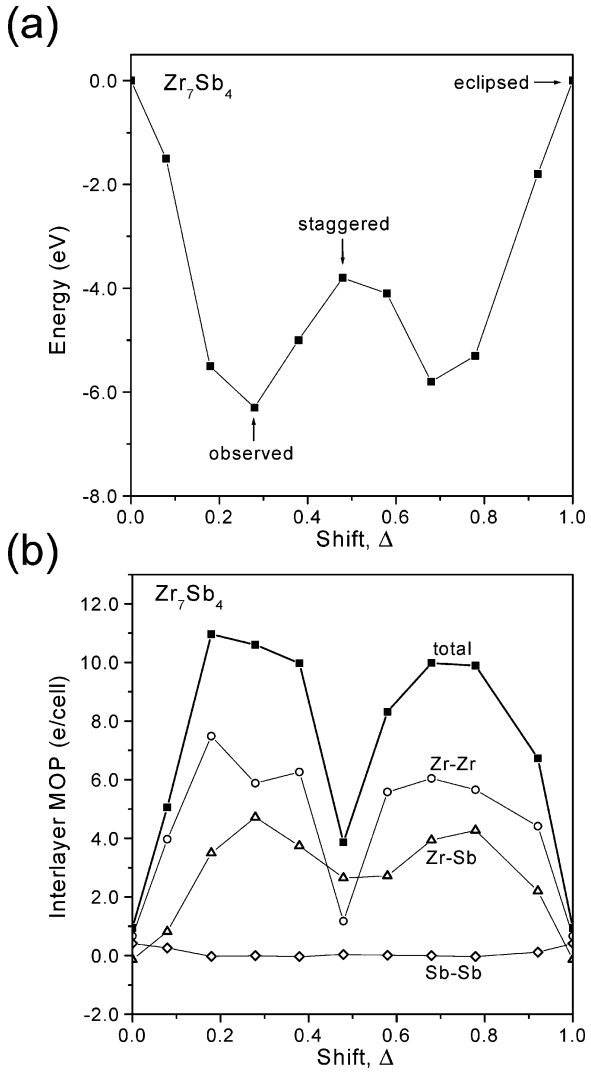

Figure 6. Plots of (a) total energy (relative to the eclipsed structure) and (b) interlayer Mulliken overlap population as a function of the shift of two-slab-thick W_5Si_3-type layers.

levels being filled, giving rise to an integrated Mulliken overlap population (MOP) of 0.311, consistent with typical values found, for example, in ZrSb.[8] Zr−Zr bonding is not quite optimized, because there are still available bonding levels above the Fermi level, but evidently a compromise must be reached so that Zr−Sb bonding is not destabilized. The shorter Zr−Zr bonds (3.0950(11)−3.2690(11) Å) are strong, with an MOP value of 0.260, but the longer contacts (3.3593(11)−3.9966(11) Å) are still significant, as anticipated, with an MOP value of 0.110. With most of the Sb−Sb antibonding levels filled, even the shortest Sb−Sb contact of 3.4587(8) Å has an MOP of only 0.016, too small to be significant.

To understand why the two-slab-thick W_5Si_3-type layers are displaced relative to each other in Zr_7Sb_4, we performed several calculations in which the shift, Δ, was varied in different model structures (Figure 2). The shift is defined in terms of fractions of the *c* parameter, with $\Delta = 0$ or 1 for an eclipsed structure and $\Delta = 0.5$ for a staggered one. The results are shown in Figure 6. The total energy of the structure oscillates from maxima at the eclipsed and staggered

structures, to minima at intermediate shifts. The lowest energy occurs at −6.3 eV (relative to the eclipsed structure), at a shift of $\Delta = 0.3$, *in agreement with the observed structure*. The other local minimum, at $\Delta = 0.7$, corresponds to a displacement of the layers in the opposite direction, which would otherwise be equivalent to the observed structure except for subtle differences in interlayer interactions arising from the nets of atoms not being rigorously planar. Plots of the integrated overlap populations for various types of interlayer interactions versus the shifts, shown in Figure 6b, reveal the origin of these energy differences. Interlayer Sb−Sb bonding is constant and negligible for all shifts. The eclipsed structure provides neither good interlayer Zr−Zr nor Zr−Sb bonding. At the other extreme, the staggered structure provides reasonably good interlayer Zr−Sb bonding, when the clusters $[Zr_{12}Sb_2]$ and $[Sb_6Zr_2]$ face across each other, but it suffers from diminished Zr−Zr bonding. Only at intermediate shifts are both Zr−Zr and Zr−Sb bonding maximized, so that clusters in one layer interact with several others in the adjacent layer. Figure 2 shows some of the strongest interlayer bonds in the observed structure.

Recognizing that Zr_7Sb_4 can be constructed from interstitial-filled square antiprismatic and tetrahedral clusters suggests that it may be worthwhile targeting the series $[M_{4(n+1)}X_n]$-$[X_{2(n+1)}M_n] = M_{5n+4}X_{3n+2}$, where Zr_7Sb_4 is the $n = 2$ member and W_5Si_3 is the $n = \infty$ member. It is likely that some of the ambiguity in the Zr−Sb system near this complicated region may be related to the formation of compounds in this series. The nearest well-identified phases, two forms of Zr_5Sb_3, do not have the W_5Si_3-type but rather the Y_5Bi_3- and Mn_5Si_3-type structures,[7] although substituted phases $Zr_5Sb_{2.5}T_{0.5}$ (T = Fe, Co, Ni, Ru, Rh) with the W_5Si_3-type structure are known.[23] It is also possible that Hf_6TiSb_4, to which Zr_7Sb_4 is isostructural, may not necessarily be a DFSO-stabilized compound, but chasing the elusive "Hf_7Sb_4" will not be trivial.

Acknowledgment. The Natural Sciences and Engineering Research Council of Canada and the University of Alberta supported this work. We thank Dr. Robert McDonald (Faculty Service Officer, X-ray Crystallography Laboratory) for the data collection and Ms. Christina Barker (Department of Chemical and Materials Engineering) for assistance with the EDX analyses.

Supporting Information Available: Crystallographic file in CIF format for Zr_7Sb_4. This material is available free of charge via the Internet at http://pubs.acs.org.

IC040034Y

(23) Kwon, Y.-U.; Sevov, S. C.; Corbett, J. D. *Chem. Mater.* **1990**, *2*, 550−556.